文章编号:1001 - 9014(2013)06 - 0486 - 05

DOI:10.3724/SP. J. 1010. 2013. 00486

Tunable diode laser absorption spectroscopy for simultaneous measurement of ethylene and methane near 1.626 μm

PAN Wei-Dong[1*], ZHANG Jia-Wei[2], DAI Jing-Min[1], ZHANG Yu-Feng[1]

(1. School of Electrical Engineering and Automation, Harbin Institute of Technology, Harbin 150001, China;
2. College of Electromechanical Engineering, Northeast Forestry University, Harbin 150040, China)

Abstract: A tunable diode laser absorption spectroscopy system with a multi pass cell and a DFB laser diode at wavelength 1.626 μm has been developed for simultaneous measurement of ethylene and methane. A line separation method based on multi absorption peak using the least squares algorithm has been established. The characteristic peak positions and relative intensities of ethylene and methane were determined by available spectral structures from previous investigations and available databases. The accuracy of the measured concentration is within 5% comparing with the mass flow meter.

Key words: TDLAS, simultaneous measurement, multi-peak

PACS: 42.62.Fi

利用可调谐半导体激光吸收光谱法在 1.626 μm 处实现乙烯和甲烷的同步检测

潘卫东[1*], 张佳薇[2], 戴景民[1], 张宇峰[1]

(1. 哈尔滨工业大学 电气工程及自动化学院,黑龙江 哈尔滨 150001;
2. 东北林业大学 机电工程学院,黑龙江 哈尔滨 150040)

摘要:研制了基于可调谐激光吸收光谱法的甲烷和乙烯的同步检测系统.该系统主要利用工作在 1.626 μm 附近的 DFB 激光器结合长光程吸收池来实现的.通过系统检测以及光谱数据库获取乙烯和甲烷在 1.626 μm 波长附近的吸收光谱信息,分析谱线的强度、位置以及相互之间的关系,采用最小二乘法建立谱线分析方法.以质量流量计为标准,系统的浓度测量精度可达到 5%.

关 键 词:TDLAS;同步检测;多峰值

中图分类号:O433.4 **文献标识码**:A

Introduction

Ethylene and methane are inflammable and will explode when mixed with air at certain concentration and ignited by naked flame[1]. They also play significant roles in atmospheric chemistry[2], global climate[3] and biological metabolism[4]. Hence, ethylene and methane detection has developed its way for high sensitivity in many application fields including atmosphere monitoring[5], coal mine fire forecasting[6], combustion process[7] and medical diagnosis for breath analysis[8].

Tunable diode laser absorption spectroscopy (TDLAS) is a valid method for non-invasive multi-compo-

Received date: 2013 - 01 - 17, **revised date**: 2013 - 09 - 05 **收稿日期**:2013 - 01 - 17, **修回日期**:2013 - 09 - 05

Foundation items: Supported by the Fundamental Research Funds for the Central Universities (DL12DB03), National Natural Science Foundation of China (60871034), and Program for New Century Excellent Talents in University (NCET-09-0279)

Biography: PAN Wei-Dong (1983-), male, Wenzhou, China, PhD candidate. Research interests include gas analysis and laser absorption spectroscopy. E-mail: whispe@163.com.

* **Corresponding author**: E-mail: whispe@163.com

nent gas analysis[9-10]. The tunable diode laser used in TDLAS has a high spectral resolution which makes it possible to scan a single absorption line of the molecule. This specific line is clearly free from the interference of other abundant species, also called "fingerprint". The diode laser working in the middle infrared range where most molecules have the fundamental vibration bands, can be used to achieve the detection limit of parts per billion (ppb) to parts per trillion (ppt) level[11-12]. Commonly, it should be refrigerated by liquid nitrogen and is expensive. The near infrared (NIR) diode laser can only access the overtone or combination bands of molecules, which are two or three orders magnitude weaker than the fundamental bands. However, a detection limit of parts per million (ppm) level can still be attained[13-14] combined with long pass cell. It has the advantage of room temperature operation, low cost and is commercially available. Additionally, it can be easily coupled to optical fibers, which makes it ideal for in-situ remote monitoring under many severe conditions[15].

In this work, we developed a TDLAS system using a NIR diode laser near 1.626 μm and measured the cross section of ethylene with it. The cross section of methane was derived from the high-resolution transmission molecular absorption database (HITRAN), where the cross section of ethylene near 1.626 μm is not recorded. Comparing the two cross sections and extracting the feature of the absorption lines, the line separation method was established based on absorption peaks using the least squares algorithm. Finally, this method was evaluated under the condition of different ratio of mixed ethylene and methane.

1 Experiments

The experimental set-up is mainly comprised of the NIR diode laser and a multi-pass cell. The scheme of the apparatus is shown in Fig. 1. A butterfly type DFB diode laser (NEL, model NLK1U5EAAA) with thermoelectric cooler inside, emitting single frequency CW radiation at 1.626 μm, was employed as the spectroscopy source. The laser is attached to a laser mount (Thorlabs, model LM14S2) which is driven by a current and temperature controller (Thorlabs, model ITC 5000). The current can be modulated from 20 Hz to 20 kHz in order to adjust the wavelength scanning rate. The laser has a pigtail fiber and its output power can reach 10mW when working at 100mA. The fiber output beam is split into two parts. One was focus on an InGaAs detector (Thorlabs, model FGA10) directly to monitor the fluctuation of laser power. The other is collimated and coupled into a multi-pass gas cell. The multi-pass cell is a White type cell[16], consisting of three spherical mirrors with same curvature radius of 200 mm. The total pass length can be adjusted by turning the angle of the mirrors. The laser beam absorbed by the gas in the cell is finally focused on another InGaAs detector. The outputs of detectors are amplified and acquired by a data acquisition card (National Instruments, model NI-DAQ 6034E) and stored in a computer operated by a LabVIEW program.

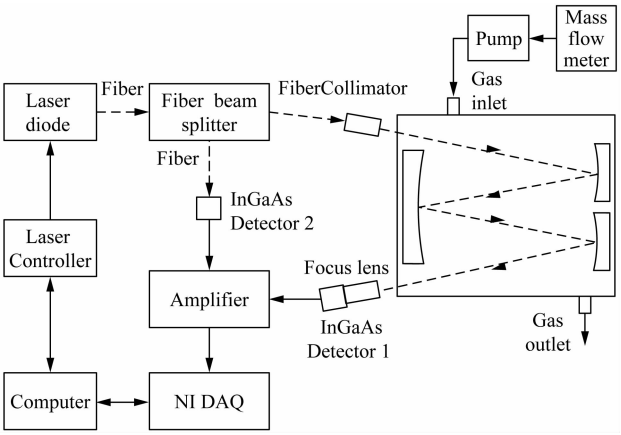

Fig. 1　Scheme of the apparatus
图 1　设备结构图

According to Beer-Lambert law, absorbed by a gas concentration of C and total path length of L, the intensity of the output beam $I_t(v)$ at wavelength v can be expressed as

$$I_t(v) = I_0(v)\exp[-\alpha(v)CL] \quad , \quad (1)$$

where $I_0(v)$ is the intensity of the input beam at wavelength v and $\alpha(v)$ is the absorption coefficient at wavelength v.

The threshold current of the DFB laser diode is 10mA. The fiber output power is 10 mW when the laser diode is operated at 25 ℃ and 100mA. The laser wavelength can be modulated either by current or by temperature. The wavelength is measured by Fourier

transform infrared spectroscopy (JASCO, model FT/IR-6000) and the wavelength error is small than 0.005 nm. The current and temperature tuning coefficients of the DFB laser diode are measured to be 0.006 nm/mA and 0.1 nm/°C respectively, shown in Fig. 2.

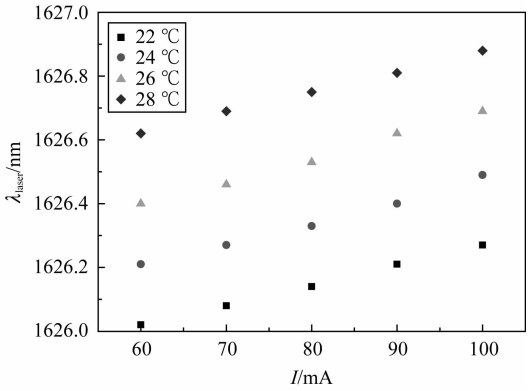

Fig. 2 Temperature and current tuning characteristics of DFB laser diode
图2 DFB半导体激光器的温度和电流调谐特性

There is none absorption data of ethylene near 1.626 μm in HITRAN, so we measured it ourselves. A frequency of 20Hz and amplitude of 20mA triangle wave was applied as the scanning wave. Meanwhile, the operation temperature of the laser diode was increased with 2℃ intervals from 20℃ to 32℃. The sampling rate was set to 200 kHz and integrating time 1s for averaging the random noise. The concentration of ethylene mixed with nitrogen was controlled to be 1% by a gas mass flow meter and the total absorption length was adjusted to 5m. The measured absorption coefficient of ethylene in the spectral range from 1.626 μm to 1.627 μm is shown in Fig. 3.

Here, we should notice the relationship and unit conversion between the absorption coefficient $\alpha(v)$ [ppm^{-1} m^{-1}] and the cross section $\sigma(v)$ [$cm^2 molecule^{-1}$],

$$\alpha(v) = N\sigma(v) \quad , \quad (2)$$

where N is the number density of the sample, and

$$N = nN_A/V \quad , \quad (3)$$

where n is the amount of gas in *mole*, $N_A = 6.022 \times 10^{23}$ [molecules·$mole^{-1}$] is the Avegadro constant and V is the volume of the gas. According to the Ideal Gas Law,

$$PV = nRT \quad , \quad (4)$$

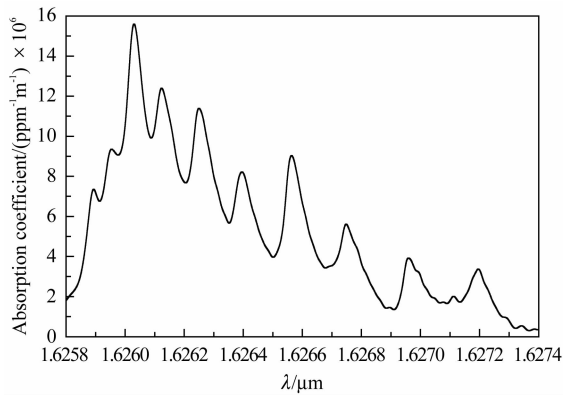

Fig. 3 Absorption coefficient of ethylene from 1.626μm to 1.627μm
图3 乙烯在1.626 μm到1.627μm处的吸收系数

where P, T are the gas pressure and temperature respectively. When the measurement is taken at 1atm pressure and 296K room temperature, the following relationship can be derived,

$$\alpha(v)\ [ppm^{-1}\ m^{-1}] = 0.24793 \times 10^{16}\ \sigma(v)\ [cm^2 molecules^{-1}] \quad . \quad (5)$$

HITRAN absorption spectra of CH_4, H_2O, CO_2, CO[17] and measured C_2H_4 in the range from 1.6258 μm to 1.6273 μm are depicted in Fig. 4. These absorption spectra show that C_2H_4 and CH_4 are interference free from other molecules that are naturally exist in the atmosphere (such as H_2O and CO_2) in this spectral range. The absorption intensity of C_2H_4 is about an order magnitude stronger than that of CH_4.

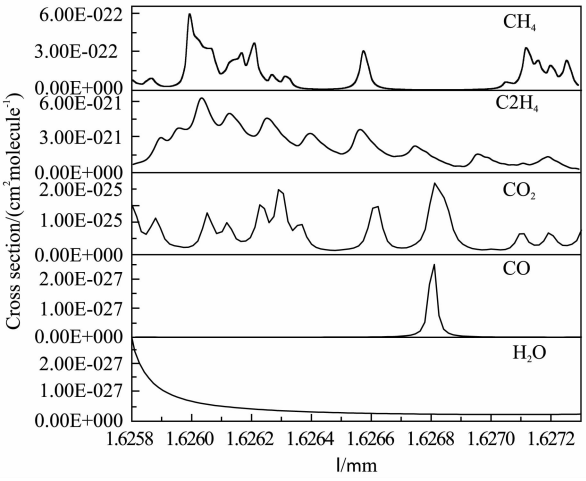

Fig. 4 Cross section of CH_4, H_2O, CO_2, CO (from HITRAN) and C_2H_4 (measured).
图4 CH_4, H_2O, CO_2, CO (来源于HITRAN数据库)和C_2H_4(测量获得)的吸收截面

When measuring multi-component gas concentration, Eq. (1) should be expressed as

$$T(v) = \ln[I_0(v)/I_t(v)] = [\alpha_1(v)C_1 + \alpha_2(v)C_2 + \cdots + \alpha_n(v)C_n]L \quad , \quad (6)$$

where n is the number of different gas. $T(v)$ is the transmission at wavelength v. All the gas shares the same optical pass, so the L is equal. In order to get the gas concentration, we pick out 13 characteristic peaks of the absorption spectra of C_2H_4 and CH_4 from Fig. 4, which are listed in Table 1.

With these peak points, Eq. (6) can be transformed into matrix form

$$T = AC \quad , \quad (7)$$

where $T = [T(v_1), \cdots T(v_i)]^T$, $C = [C_1, \cdots, C_n]^T$, $A = [\alpha_1, \cdots, \alpha_n]$, $\alpha = [\alpha(v_1), \cdots \alpha(v_i)]^T$. In this experiment, $i = 13$ and $n = 2$. According to least squares algorithm,

$$C = (A^TA)^{-1}A^TT \quad . \quad (8)$$

Table 1　Characteristic peak positions and intensities
表 1　特征峰位置和强度

Peak position/μm	Peak intensity ×10^20/ (cm²molecule⁻¹)		Peak position/μm	Peak intensity ×10^20/ (cm²molecule⁻¹)	
	C_2H_4	CH_4		C_2H_4	CH_4
1.62600	0.397	0.0590	1.62659	0.313	0.0305
1.62604	0.633	0.0373	1.62676	0.228	0.0006
1.62613	0.503	0.0189	1.62697	0.159	0.0006
1.62622	0.322	0.0365	1.62715	0.073	0.0329
1.62626	0.462	0.0091	1.62720	0.137	0.0166
1.62640	0.333	0.0012	1.62729	0.040	0.0231
1.62657	0.367	0.0086			

2　Results and discussion

The simultaneous measurement of ethylene and methane was carried out at 1atm pressure and 296 K room temperature. A multi pass cell was used with total absorption length of 5m. Before pumping the mixed gas, we swept the cell with high purity nitrogen gas (99%) for about 15 minutes to make the cell clear. The mixed gas of different concentration was controlled by a mass flow meter at a constant rate also for 15 minutes to get a stable concentration matching with the controller.

Figure 5 illustrates the measured and the calculated transmission together with the residual error of the two. The concentration results are shown in Table 2 and the relative errors are within 5%. Using the characteristic absorption peaks to fit the measured transmission of the multi-component gas is a simple and efficient way to get the component concentration.

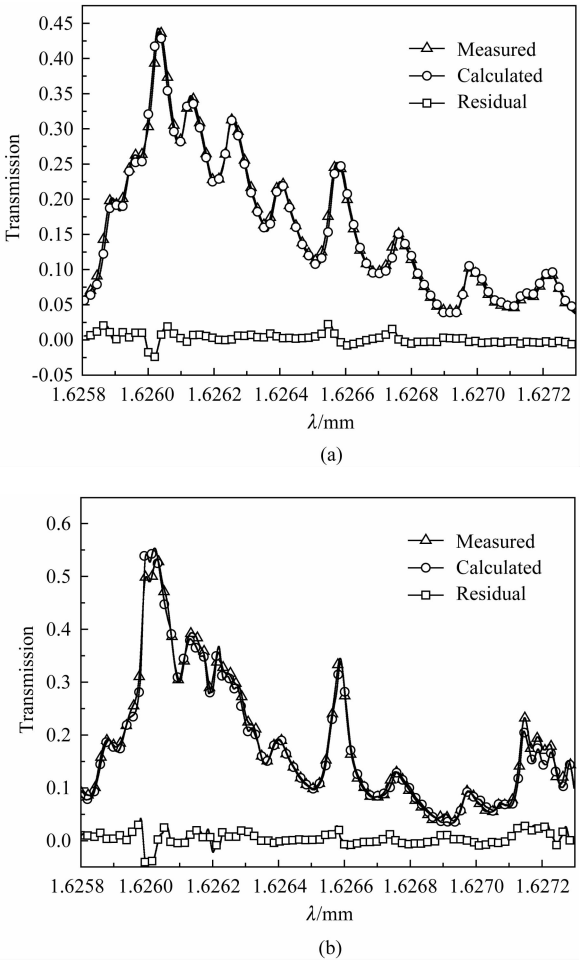

Fig. 5　The measured (open triangles) and the calculated (open circles) transmission by multi-peak fit algorithm and their residual error (open squares). (a) The absorption intensity of ethylene is much stronger than methane, (b) The absorption intensity of ethylene and methane is equivalent
图 5　测量结果(三角形)与多峰值拟合算法计算值(圆形)及其偏差(方形)(a) 乙烯的吸收强于甲烷, (b) 乙烯与甲烷的吸收强度相当

Table 2　Concentration measurement result and comparison with the mass flow meter
表 2　浓度测量结果及其与质量流量计的比较

Controlled concentration /%		Measured concentration /%		relative error /%	
C_2H_4	CH_4	C_2H_4	CH_4	C_2H_4	CH_4
0.55	0.5	0.534	0.481	-2.86	-3.86
0.53	1.1	0.520	1.054	-1.87	-4.20
0.51	1.6	0.507	1.680	1.40	4.98
0.46	4	0.452	4.084	-1.83	2.10

3　Conclusions

This apparatus has been proved to be efficient for simultaneous concentration measurement of ethylene

and methane based on TDLAS near 1.626 μm. The determined characteristic peak positions from previous investigations and available databases are reasonable for separating the mixed gas absorption line. A measurement accuracy of 5% can be achieved as verified with the standard sample of mixed controlled concentrations.

REFERENCES

[1] Schoor F V, Verplaetsen E, Berghmans J. Calculation of the upper flammability limit of methane/air mixtures at elevated pressures and temperatures[J]. *J. Hazard. Mater.*, 2008, **153**(3):1301-1307.

[2] Rice C A, Perram G. A tunable diode laser absorption system for long path atmospheric transmission and high energy laser applications[C]. *In atmospheric and oceanic propagation of electromagnetic waves V*, *SPIE*, 2011:7924.

[3] Polson D, Fowler D, Nemitz E, *et al*. Estimation of spatial apportionment of greenhouse gas emissions for the UK using boundary layer measurements and inverse modelling technique[J]. *Atmos. Environ.*, 2011, **45**(4):1042-1049.

[4] Giubileo G, Dominicis L D, Fantoni R, *et al*. Photoacoustic detection of ethylene traces in biogenic gases[J]. *Laser Phys.*, 2002, **12**(4):653-655.

[5] Basu S, Lambe D E, Kumar R. Water vapor and carbon dioxide species measurements in narrow channels[J]. *Int. J. Heat Mass Transfer*, 2010, **53**(4):703-714.

[6] Adamus A, Sancer J, Guranova P, *et al*. An investigation of the factors associated with interpretation of mine atmosphere for spontaneous combustion in coal mines[J]. *Fuel Process. Technol.*, 2011, **92**(3):663-670.

[7] Hendricks A G, Vandsburger U, Saunders W R, *et al*. The use of tunable diode laser absorption spectroscopy for the measurement of flame dynamics[J]. *Meas. Sci. Technol.*, 2006, **17**(1):139-144.

[8] Puiu A, Giubileo G, Bangrazi C. Laser sensors for trace gases in human breath[J]. *Intern. J. Environ. Anal. Chem.*, 2005, **85**(12-13):1001-1012.

[9] McCulloch M T, Langford N, Duxbury G. Real-time trace-level detection of carbon dioxide and ethylene in car exhaust gases[J]. *Appl. Opt.*, 2005, **44**(14):2887-2894.

[10] Boschetti A, Bassi D, Iacob E, *et al*. Resonant photoacoustic simultaneous detection of methane and ethylene by means of a 1.63-μm diode laser[J]. *Appl. Phys. B*, 2002, **74**(3):273-278.

[11] Harward C N, Thweatt W D, Baren R E, *et al*. Determination of molecular line parameters for acrolein(C3H4O) using infrared tunable diode laser absorption spectroscopy[J]. *Spectrochim. Acta. Part A*, 2006, **63**(5):970-980.

[12] Krzempek K, Lewicki R, Nahle L, *et al*. Continuous wave, distributed feedback diode laser based sensor for trace-gas detection of ethane[J]. *Appl. Phys. B*, 2012, **106**(2):251-255.

[13] Duraev V P, Marmalyuk A A, Petrovskiy A V. Tunable laser diodes for the 1250 ~ 1650 nm spectral range[J]. *Spectrochim. Acta. Part A*, 2007, **66**(4-5):846-848.

[14] Guan Z, Lewander M, Svanberg S. Quasi zero-background tunable diode laser absorption spectroscopy employing a balanced Michelson interferometer[J]. *Opt. Express*, 2008, **16**(26):21714-21720.

[15] Brown D M, Shi K B, Liu Z W, *et al*. Long-path supercontinuum absorption spectroscopy for measurement of atmospheric constituents[J]. *Opt. Express*, 2008, **16**(12):8457-8471.

[16] Mazzotti D, Giusfredi G, Cancio P, *et al*. High-sensitivity spectroscopy of CO_2 around 4.25 μm with difference-frequency radiation[J]. *Opt. Laser Eng*, 2002, **37**(2):143-158.

[17] Rothman L S, Gordon I E, Barbe A, *et al*. The HITRAN 2008 molecular spectroscopic database[J]. *J. Quant. Spectrosc. Radiat. Transfer*, 2009, **110**(40462):533-572.

(上接485页)

GaAs quantum wells with type-I emission beyond 3μm[J]. *Appl. Phys. Lett.*, 2011, **99**(8): 081914.

[4] Hudait M K, Lin Y, Ringel S A. Strain relaxation properties of $InAs_yP_{1-y}$ metamorphic materials grown on InP substrates[J]. *J. Appl. Phys*, 2009, **105**(6): 061643.

[5] Kirch J, Garrod T, Kim S, *et al*. $InAs_yP_{1-y}$ metamorphic buffer layers on InP substrates for mid-IR diode lasers[J]. *J. Cryst. Growth*, 2010, **312**(8): 1165 - 1169.

[6] Tångring I T, Wang S M, Zhu X R, *et al*. Manipulation of strain relaxation in metamorphic heterostructures[J]. *Appl. Phys. Lett*, 2007, **90**(7): 071904.

[7] Song Y X, Wang S M, Lai Z H, *et al*. Enhancement of optical quality in metamorphic quantum wells using dilute nitride buffers[J]. *Appl. Phys. Lett*, 2010, **97**(9): 091903.

[8] Yang J, Bhattacharya P, Mi Z. High-performance $In_{0.5}Ga_{0.5}As$/GaAs quantum-dot lasers on silicon with multiple-layer quantum-dot dislocation filters[J]. *IEEE Trans. Electron Devices* 2007, **54**(11): 2849 - 2855.

[9] Gu Y, Zhang Y G., Wang K, *et al*. InAlAs graded metamorphic buffer with digital alloy intermediate layers[J]. *Jpn. J. Appl. Phys*, 2012, **51**(8): 080205.

[10] Tersoff J. Dislocations and strain relief in compositionally graded layers[J]. *Appl. Phys. Lett.*, 1993, **62**(7): 693 - 695.

[11] Zhang Y G., Gu Y, Wang K, *et al*. Properties of gas source molecular beam epitaxy grown wavelength extended InGaAs photodetectors structures on linear graded InAlAs buffer[J]. *Semicon. Sci. Technol*, 2008, **23**(12): 125029.

[12] Lee D, Park M S, Tang Z, *et al*. Characterization of metamorphic $In_xAl_{1-x}As$/GaAsbuffer layers using reciprocal space mapping[J]. *J. Appl. Phys*, 2007, **101**(6): 063523.

[13] Choi H, Jeong Y, Cho J, *et al*. Effectiveness of non-linear graded buffers for In(Ga, Al)As metamorphic layers grown on GaAs (0 0 1)[J]. *J. Cryst. Growth*, 2009, **311**(4): 1091 - 1095.

[14] Wang K, Zhang Y G, Gu Y, *et al*. Improving the performance of extended wavelength InGaAs photodetectors by using digital graded hetero-interfaces superlattice[J]. J. Infrared Millim. Waves., 2009, **28**(6): 0405.